Roughness in the periodic potential induces absolute negative mobility in a driven Brownian ratchet

Archana G. R. and Debashis Barik*
School of Chemistry, University of Hyderabad, Gachibowli, 500046 Hyderabad, India

(Received 18 August 2022; accepted 3 October 2022; published 21 October 2022)

Absolute negative mobility, where particles move opposite to the direction as governed by the external load, is an anomalous transport property of a Brownian ratchet and has technological implications in mass separation and bioanalytical applications. We numerically investigated here the effect of roughness in symmetric periodic potential on the negative mobility of a driven inertial Brownian ratchet in the presence of an external load. We show that the microscopic spatial heterogeneity of the potential can generate negative mobility which would not otherwise be possible under smooth potential in the concerned parameter space. We determined the optimal condition in terms of parameter space for such anomalous behavior. Our calculations indicate that the shift of balance towards the negative velocity phase in the temporal oscillations of velocity and weakly chaotic dynamics are responsible factors for roughness-induced negative mobility. These calculations highlight a constructive role of roughness in the anomalous transport properties of Brownian ratchet.

DOI: 10.1103/PhysRevE.106.044129

I. INTRODUCTION

Over the past few decades, a plethora of studies have been carried out to understand the transport properties of nonequilibrium systems such as Brownian ratchets[1–5]. Brownian ratchets are a class of systems that generate directed motion from unbiased nonequilibrium fluctuations by breaking the spatial symmetry and the principle of detailed balance. Rocking ratchet, flashing ratchet, diffusion ratchet and correlation ratchet are some of the important examples of extensively studied Brownian ratchet models that function far from equilibrium [3,5]. Absolute negative mobility (ANM) is an anomalous feature in transport of Brownian ratchets and it is characterized by a net current of mass in the direction opposite to the direction of the external load [6–16]. At equilibrium such a physical phenomena will be contradictory to Newton's laws of motion; however, in nonequilibrium condition negative mobility has been observed in many experimental systems. Experimentally it has been observed in a variety of quantum mechanical systems such as the nonlinear response in p-modulation-doped quantum wells [17], absolute negative conductance in semi-conductor super lattices [18,19], absolute negative resistance in a two-dimensional electron gas [20], negative absolute resistance in a Josephson Junction [21]. ANM has also been observed in classical systems such as in charged colloidal particles in microfluidic channels [22,23]. ANM has potential technological applications such as separation of particles based on their mass [24–26].

Spatially periodic potential in the Brownian ratchet is a key ingredient in the transport of the particle and various types of model potential have been explored Brownian ratchets [5]. Traditionally a smooth periodic potential devoid of any spatial heterogeneity has been the choice in exploring the transport properties of Brownian particles. However, microscopic spatial heterogeneity in potential landscape is known to exist in many physical and chemical systems. For example, multiple microscopic local minima are known to present between two global attractor states in the protein folding pathway and such microscopic minima creates spatial heterogeneity in the potential landscape [27–29]. Metabasins which are microscopic fine structures in the free energy landscape is known to cause slow diffusion in structural glasses [30,31]. Highly viscous properties of supercooled glasses and liquids are attributed to rough potential energy landscape [32,33]. In bacteria membrane transport of ions through the ion channels are also regulated by spatially heterogeneous energy landscape [34].

In the context of Brownian ratchet, the effect of roughness was investigated on an over-damped thermal ratchet to find that roughness works as a hindrance to the transport supporting the early finding of Zwanzig on the estimation of first passage time across rough potential barrier [35,36]. However, more recent findings shows that roughness enhances transport in both over-damped and inertial systems under Levy noise and it was argued that the microscopic heterogeneity of the potential ladders up the particle through the barrier resulting in enhanced transport [37–39]. Recently we have shown that in the weak noise limit, small roughness in the asymmetric periodic potential leads to enhancement of transport as compared to the smooth potential for driven inertial Brownian ratchet [40].

In the present work, we studied the transport properties of a driven inertial Brownian particle under a symmetric rough periodic potential in the presence of an external load. Due to the potential technological applications of ANM in the context of mass separation, our objective was to investigate the fate of ANM under the roughness of the periodic potential in a driven inertial ratchet under an external load. We found that ANM can be established purely by the roughness of the potential in a moderately weak noise limit. We determined the optimal

*dbariksc@uohyd.ac.in

parameter range where the extent of ANM was maximum. We attributed to such anomalous behavior of transport to the shift in the balance of average duration of negative and positive phases in the oscillations of velocity. Further, our calculations indicate that weak deterministic chaos may also be a responsible factor for the roughness-induced ANM. In Sec. II the model of the driven Brownian ratchet under a rough symmetric periodic potential in the presence of an external load is described. The results are described in Sec. III and we summarize the work in Sec. IV.

II. MODEL

We have considered a classical Brownian particle of mass M under a spatially symmetric rough periodic potential $U(x)$ along with an external load F and the particle is driven out of equilibrium by an unbiased time-periodic force $A\cos(\Omega t)$ with an amplitude A and an angular frequency Ω. The Langevin equation of the particle is given by

$$M\ddot{x} = -U'(x) + F + A\cos(\Omega t) - \Gamma\dot{x} + \xi(t). \tag{1}$$

The $(\cdot)$ and $(')$ above x denote derivative with respect to time, t, and position, x, respectively. The fourth and the fifth terms on the right-hand side of the above equation are frictional force and thermal fluctuations, respectively, originating from the heat bath where the particle is immersed into. The thermal noise, $\xi(t)$, is Gaussian, unbiased $\langle\xi(t)\rangle = 0$, and follows the fluctuation-dissipation relation, $\langle\xi(t)\xi(t')\rangle = 2\Gamma k_B T\delta(t-t')$, where Γ, k_B and T represent the frictional coefficient, the Boltzmann constant and the temperature, respectively.

The symmetric periodic potential $U(x)$ consists of a large amplitude low frequency $U_0(x)$ and small amplitude large frequency $U_1(x)$ terms and it is given as

$$U(x) = U_0(x) + U_1(x). \tag{2}$$

The $U_0(x)$ represent smooth part of the periodic potential and was chosen as

$$U_0(x) = -\Delta U\sin\left(\frac{2\pi}{L}x\right), \tag{3}$$

with L as the periodicity and ΔU as the barrier height. To achieve roughness in the potential, $U_1(x)$ was superposed with the smooth potential $U_0(x)$ and was chosen as [36]

$$U_1(x) = \Delta U\epsilon_0\cos(\Lambda x), \tag{4}$$

where ϵ_0 is the amplitude of the roughness and Λ is the periodicity of the rough part of the potential. Typically the periodicity of smooth part is much larger than that of the rough part of the potential. To reduce the number of variables, we nondimensionalized Eq. (1) and the dimensionless version of the equation of motion is given as [15]

$$\ddot{\hat{x}} = -\hat{U}'(\hat{x}) + f + a\cos(\omega\hat{t}) - \gamma\dot{\hat{x}} + \hat{\xi}(\hat{t}). \tag{5}$$

The $\hat{x}(=2\pi x/L)$ and $\hat{t}(=t/\tau_0)$ are the dimensionless position and time, respectively, with $\tau_0 = \frac{L}{2\pi}\sqrt{M/\Delta U}$. The other parameters are rescaled as $\gamma = \tau_0\Gamma/M$, $a = AL/2\pi\Delta U$, $f = FL/2\pi\Delta U$, $Q = k_BT/\Delta U$, $\epsilon = \epsilon_0/\Delta U$, $\lambda = \Lambda L/2\pi$, and $\omega = \tau_0\Omega$. The rescaled thermal noise is $\hat{\xi}(\hat{t})$ $[= (L/2\pi\Delta U)\xi(\tau_0\hat{t})]$ and follows the following relations

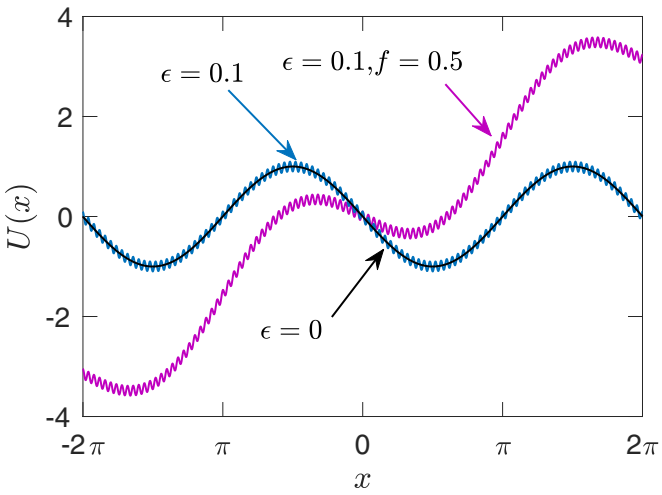

FIG. 1. Schematic representation of symmetric periodic potential, $U(x)$, without and with roughness and load.

$\langle\hat{\xi}(\hat{t})\rangle = 0$ and $\langle\hat{\xi}(\hat{t})\hat{\xi}(\hat{t}')\rangle = 2\gamma Q\delta(\hat{t}-\hat{t}')$. The dimensionless potential is given by $\hat{U}(\hat{x}) = U((L/2\pi)x)/\Delta U$ possesses the period $L = 2\pi$. The rescaled potential is now given as

$$\hat{U}(\hat{x}) = -\sin(\hat{x}) + \epsilon\cos(\lambda\hat{x}). \tag{6}$$

The parameter ϵ determines the amplitude of roughness of the periodic potential. We set the value of λ as 50 throughout the paper. Figure 1 shows the smooth ($\epsilon = 0$) and rough periodic ($\epsilon = 0.1$) potential with ($f = 0.5$) and without ($f = 0$) the external load.

To determine transport properties of the Brownian particle under rough symmetric periodic potential in presence of an external load, we computed the asymptotic ensemble and period average velocity, $\langle v\rangle$, defined as [41]

$$\langle v\rangle = \lim_{t\to\infty}\frac{1}{T}\int_t^{t+T} ds\langle\dot{x}(s)\rangle. \tag{7}$$

The angular bracket, $\langle\rangle$, represents the ensemble average over many different initial x and $\dot{x}$. The period average was preformed over a period ($T = 2\pi/\omega$) of the external driving force. We numerically integrated the Langevin equation (5) using second-order predictor-corrector method with randomly chosen initial values of x and $\dot{x}$, and the values were sampled from uniform distributions over the interval $[0, 2\pi]$ and $[-2, 2]$, respectively, for the x and $\dot{x}$. Due to the short periodicity of the rough part of the potential, we chose a very small step size $10^{-4}\times\frac{2\pi}{\omega}$ in the calculations. In all calculations, simulations were carried out for a total time of $10\,000\times T$ and ensemble averaging were carried out over 2048 initial conditions. We calculated $\langle v\rangle$ using Eq. (7) where we first averaged the velocity over a period in the long time limit and finally averaged the resultant over an ensemble of trajectories. In addition we also calculated $\langle v\rangle$ from the $x(t)$ of the particle. Here we subtracted the position at a transient time ($t = 20T$) from the position at the final time ($t = 10\,000T$) and dividing the difference by the time interval and finally averaging the resultant over an ensemble of trajectories. We showed that both the methods leads to identical outcomes [Figs. 2(a) and 2(b)]. We point out here that calculation of $\langle v\rangle$

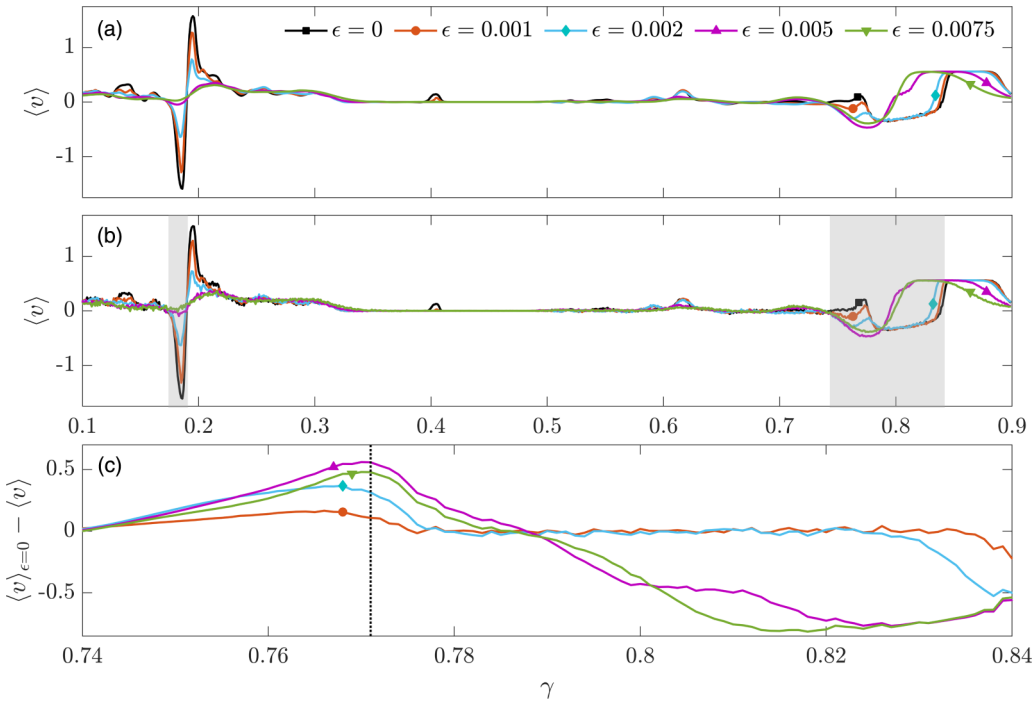

FIG. 2. The ensemble and period-average velocity calculated from $x(t)$ (a) and $\dot{x}(t)$ (b) as a function of γ for different values of ϵ. The shaded part indicate the region of γ where the system shows ANM. (c) The plot of difference between the $\langle v \rangle$ without and with roughness ($\langle v \rangle_{\epsilon=0} - \langle v \rangle$) with γ. The vertical line represents maximum difference between the $\langle v \rangle$ without and with roughness. Other parameters were $f = 0.015$, $Q = 0.00035$, $a = 1.589$, and $\omega = 0.559$.

from the position is computationally slightly less expensive as compared to the first method as the first method requires greater ensemble averaging to minimize fluctuation.

III. RESULTS AND DISCUSSIONS

The dynamics of the driven inertial ratchet is governed by a six-dimensional parameter space (ϵ, a, ω, γ, f, Q). Previous studies have shown the importance of the parameters in dictating the nontrivial behavior of the similar system under smooth periodic potential [42]. As our objective is to determine a condition of roughness-induced ANM, we first determined the parameter space relevant to the anomalous negative mobility of the system by numerically scanning the parameters individually. Figure 2(a) shows the dependence of $\langle v \rangle$, calculated from $x(t)$, on the dissipation constant, γ, for different degrees of the roughness, ϵ, at a particular value of external load, $f = 0.015$. Figure 2(b) shows $\langle v \rangle$ versus γ plot where $\langle v \rangle$ was calculated using Eq. (7). The visual comparison of these two plots points out nearly identical outcomes from both the methods. The variation of $\langle v \rangle$ with γ for different values of the ϵ underscores the parametric dependence of ANM. There are two regions (shaded areas) where the system exhibits ANM. The region on the left, the system shows ANM under the smooth potential and with roughness the extent of ANM decreases. Although in the region on the right both the rough ($\epsilon \neq 0$) and smooth ($\epsilon = 0$) systems exhibit ANM and, however, there is a region of γ where ANM is purely due to roughness in the potential as the smooth system results in positive values of $\langle v \rangle$ against a positive load of $f = 0.015$. Thus, there is a region of γ where ANM can be driven only by the microscopic spatial heterogeneity of the potential. To determine the value of γ where the extent of roughness-driven ANM is maximum, we calculated the difference of $\langle v \rangle$ between the smooth and rough systems and determined the value of γ corresponding to the maximum in the difference [Fig. 2(c)]. We followed similar procedure to identify the values of amplitude (a) and frequency (ω) of the external driving force [Figs. 3(a) and 3(b)]. These calculations also highlight that there are regions of parameter values where the system does not show any directed transport. Thus, even for normal transport against the external load an optimal combination of all parameters are necessary. Based on these calculations we fixed the values of the γ, a, and ω as 0.771, 1.589, and 0.558, respectively, for the subsequent calculations.

After determining the initial parameter space corresponding to roughness-driven ANM, we investigated the effect of the external load on the anomalous nature of the transport across different degrees of the roughness. Figure 4(a) shows $\langle v \rangle$ as a function of load, f, for different values of ϵ at a particular value of noise intensity, Q. It indicates that the the system does not exhibit anomalous transport across a large range of load under the smooth potential ($\epsilon = 0$). However, with the introduction of roughness the system exhibits ANM that increases with the load and with subsequent increase of load the particle changes the direction of the current from negative to positive leading to current reversal. The extent of ANM increases initially with roughness (more negative $\langle v \rangle$); however, at a large roughness the system does not show ANM. Thus, introduction of roughness in the periodic potential leads to two key aspects of transport—anomalous transport and current reversal. It further points out that there

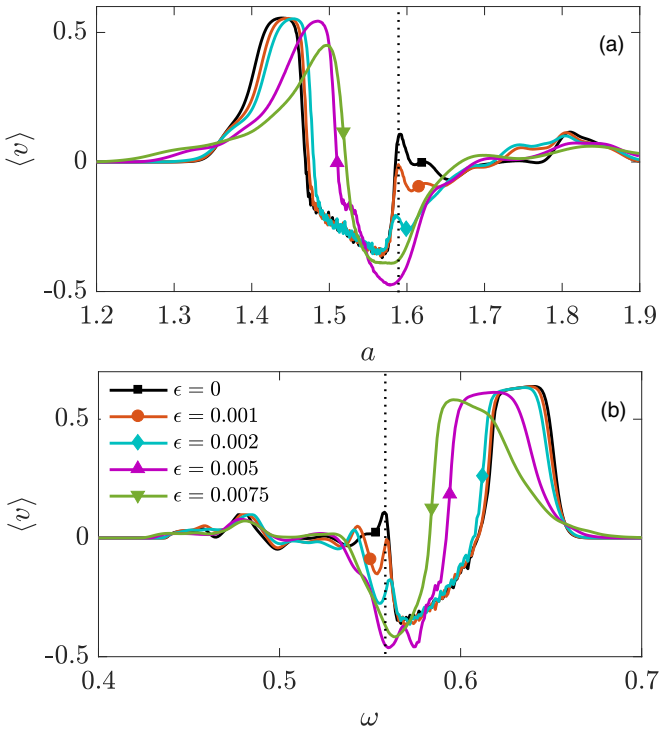

FIG. 3. Parameter scanning for amplitude, a (a), and frequency, ω (b), of the external driving force. The values of γ, Q, and f were 0.771, 0.00035, and 0.015, respectively. In the scans of a and ω, ω and a were chosen to be 0.558 and 1.589, respectively. The vertical lines represent the selected values of the respective parameters where the difference between the average velocities without and with roughness was maximum.

is an optimal roughness where the system exhibits maximum ANM. Across various values of ϵ, the load corresponding to maximum negative average velocity was determined to be at $f \approx 0.03$. Repeat of these calculations for increasing values of the noise strength show that [Figs. 4(c) and 4(d)] the ANM and current reversal diminishes with in the regime of large noise. Particularly the range of load for which the system exhibits ANM decreases with the increase of Q. It is important to note that the transport property of the system under smooth potential remains somewhat unaltered across different values of noise strength. Thus it seems that the roughness-induced ANM and current reversal is a property of the system in the weak noise limit. This finding is consistent with our previous observation that enhancement of transport of particle occurs only in the limit of weak noise in the context of transport under asymmetric periodic potential [40].

Our calculations show that roughness-induced ANM is observed at a smaller amplitude of roughness along with a smaller range of positive load. It is possible that the small amplitude roughness in the potential energy acts as a hindrance to the movement of the particle in the small positive range of load and thereby forcing the particles to move in the opposite direction leading to negative mobility. To verify that, we calculated $\langle v \rangle$ in the negative range of load for the same domain of roughness as well as other parameters (Fig. 5). In the small negative load region, the direction of the current is opposite to the direction of the load indicating that the small

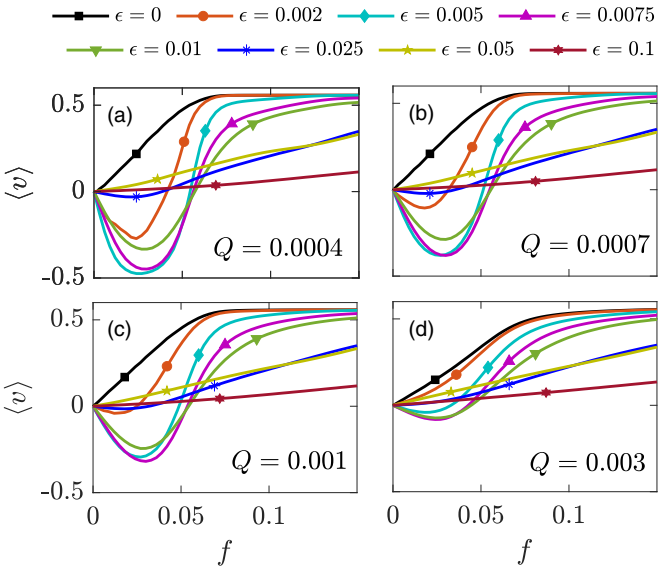

FIG. 4. The variation of $\langle v \rangle$ as a function of external load, f, for different values of Q and ϵ. Other parameters were $\gamma = 0.771$, $a = 1.589$, and $\omega = 0.558$.

amplitude roughness force the particles to move against the direction of the load in the small load region.

Next we studied the dependence of the $\langle v \rangle$ on the ϵ at a load corresponding to the maximum negative velocity (f corresponding to minimum in the Fig. 4) at different value of Q (Fig. 6). Across different noise strengths, in the limit of $\epsilon = 0$ the system exhibits normal transport and with increasing roughness it shows negative average velocity that decreases sharply with the increase of ϵ. With subsequent increase of roughness, the value of negative current deceases and direction of the current becomes positive and in the large roughness limit it becomes negative again. Therefore, the system undergoes multiple current reversal with the increasing value of ϵ.

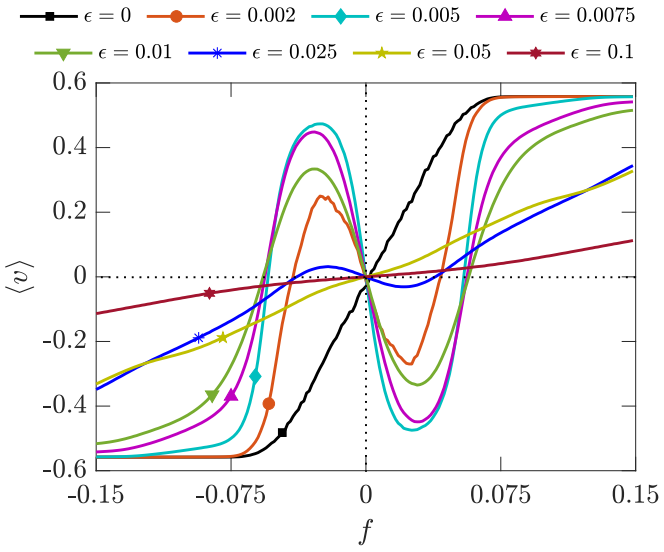

FIG. 5. The plot of $\langle v \rangle$ as a function of external load, f, at $Q = 0.0004$ for different values of ϵ. Other parameters were the same as in Fig. 4.

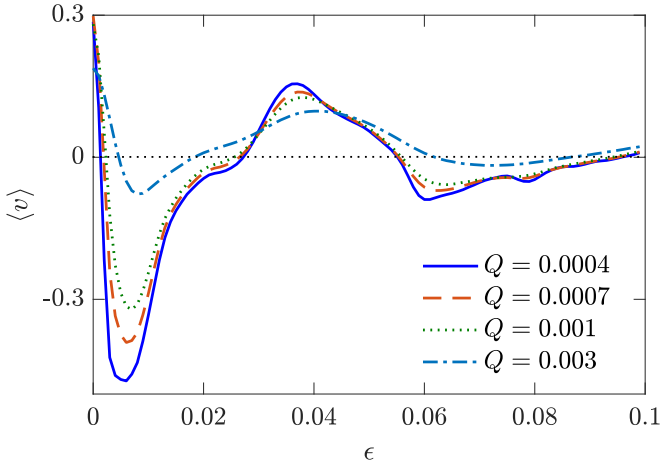

FIG. 6. The variation of $\langle v \rangle$ as a function of ϵ for different values of Q. Other parameters were the same as in Fig. 4.

The extent of ANM is more in the limit of small value of Q. To find out the fate of ANM across a large range of noise strength, we calculated $\langle v \rangle$ as a function of Q for different values of ϵ (Fig. 7) at an external load ($f = 0.03$) corresponding to the maximum ANM as indicated in the Fig. 4. In the very weak noise limit ($Q < 0.0002$), the system under smooth potential exhibits ANM. With the introduction of a small roughness, the extent of ANM increases; however, large roughness forces the particle to move along the direction of the external load diminishing the ANM. In the intermediate region of the noise strength ($0.0002 < Q < 0.003$), only the rough system moves opposite to the direction of the load exhibiting substantial amount of ANM. In the large noise limit the system does not exhibit ANM at all. Therefore, in an intermediate range of noise strength ANM can be observed due to the roughness of the potential energy.

Previously the direction of current have been associated to the direction of the running states of the trajectories[7,43].

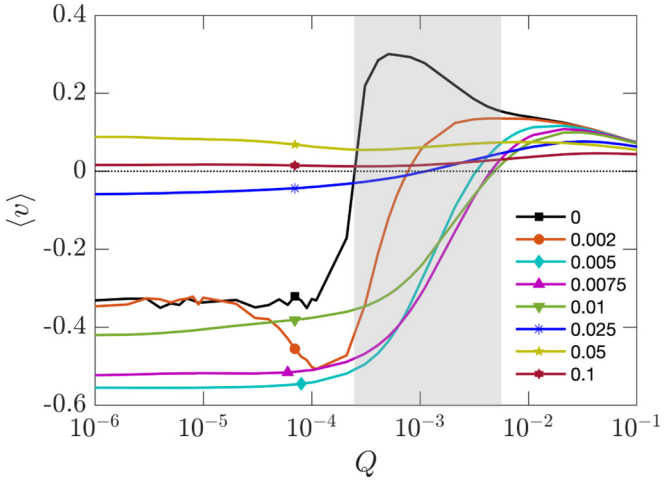

FIG. 7. The variation of $\langle v \rangle$ as a function of Q for the indicated values of ϵ. The shaded part indicates the region of Q where roughness-driven ANM occurs. Other parameters were the same as in Fig. 4.

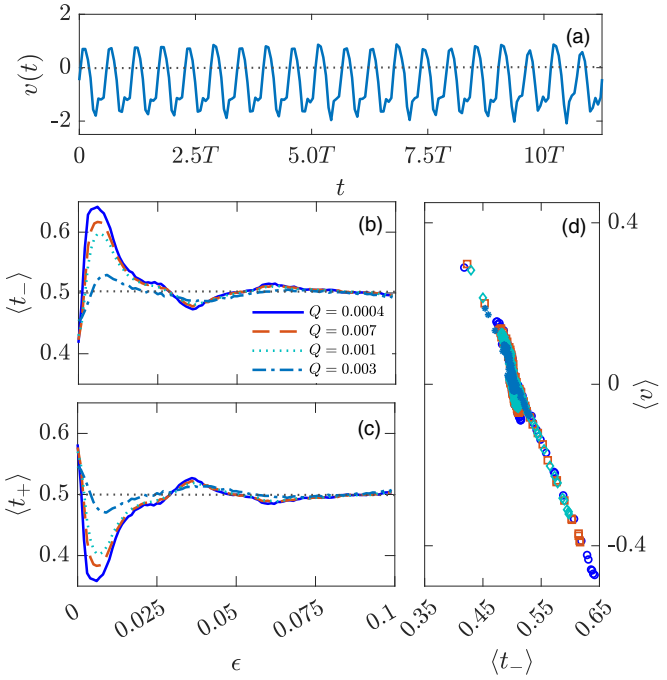

FIG. 8. Temporal oscillation of velocity, $\dot{x}(t)$ (a). The average fraction of time with negative ($\langle t_- \rangle$) and positive ($\langle t_+ \rangle$) velocity in $\dot{x}(t)$ during onefull time period (T) of external driving are plotted as a function of ϵ for different values of Q (b, c). The correlation plots of $\langle v \rangle$ with $\langle t_- \rangle$ for different values of Q. Other parameters were the same as in Fig. 4.

Typically with a net nonzero average velocity, $x(t)$ exhibits a running state defined as the increasing (or decreasing) values of x with time. However, irrespective of the value of the current, $\dot{x}(t)$ oscillates over time due to the periodic driving force [Fig. 8(a)]. To make an association between the ANM and the dynamics of the system, we calculated the average fraction of duration the system spends with positive ($\langle t_+ \rangle$) or negative ($\langle t_- \rangle$) velocities during a full time period of the external driving (T). Intuitively, if the system spends more time in the negative velocity phase then the sign of the $\langle v \rangle$ must be negative. Therefore, the sign of the current must be predicted from by looking into either $\langle t_- \rangle$ or $\langle t_+ \rangle$. Figure 8(b) shows the variation of the $\langle t_- \rangle$ with ϵ and it indicates that the increase in $\langle t_- \rangle$ leads to the increase in the average negative velocity (Fig. 6). Therefore, its variation with ϵ is consistent with the $\langle v \rangle$ versus ϵ plot in Fig. 5. Consequently, $\langle t_+ \rangle$ behaves in a complementary manner [Fig. 8(c)]. $\langle v \rangle$ shows a good correlation with t_- and large negative $\langle v \rangle$ strongly correlates with the large $\langle t_- \rangle$ [Fig. 8(d)]. These suggest that the shifts in the balance of positive and negative velocity phases in the temporal oscillation of $\dot{x}(t)$ ultimately dictates the direction of the average current in the transport.

Previous works have suggested chaotic dynamics as the origin for the ANM [7,8,44]. To determine any potential role of chaotic dynamics in generating ANM, we calculated the bifurcation diagram where the maximum of the temporal velocity, $\dot{x}_{\max}$, is plotted against the roughness parameter, ϵ, for the deterministic ($Q = 0$) dynamical system (Fig. 9). With ϵ, the chaotic nature of the system varies quite extensively.

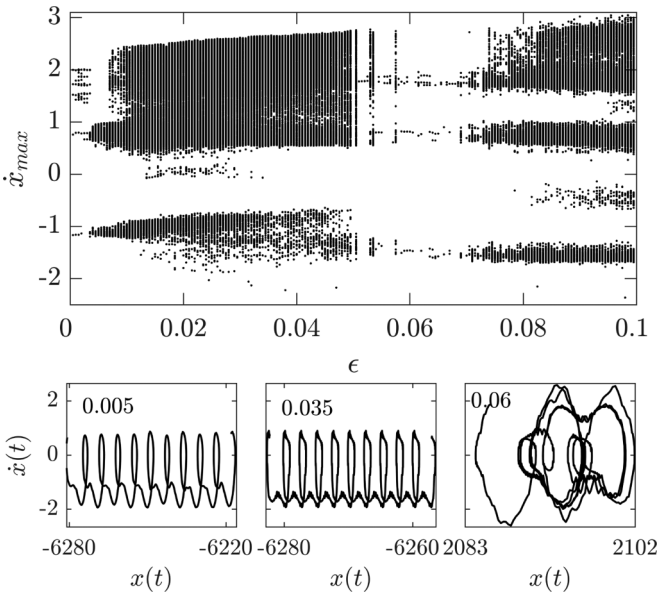

FIG. 9. Bifurcation diagram ($\dot{x}_{\max}$ vs ϵ) of the deterministic dynamical system with $Q = 0.0$ and $f = 0.03$ (top panel). Representative phase-space plots for the indicated values of ϵ (bottom panel).

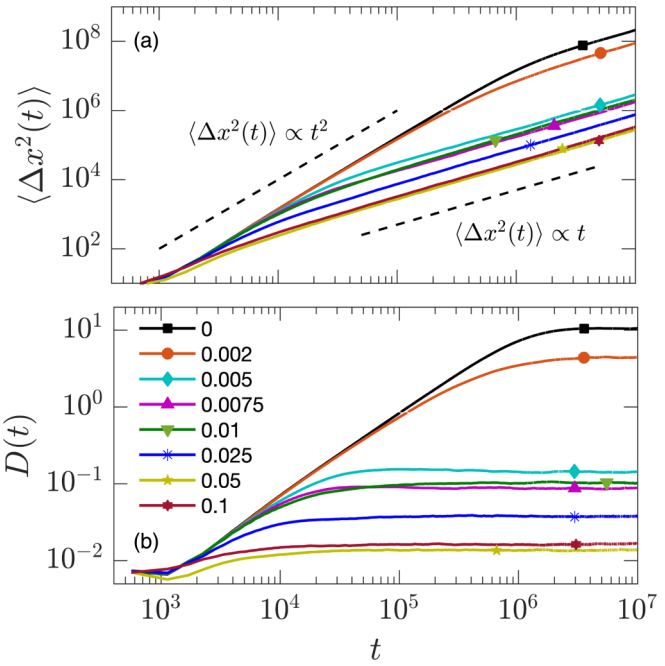

FIG. 10. (a) The plot of mean square displacement, $\langle \Delta x^2(t) \rangle$, as a function of time for different values of ϵ. The ballistic diffusion ($\langle \Delta x^2(t) \rangle \propto t^2$) in the early phase and normal diffusion in the later phase ($\langle \Delta x^2(t) \rangle \propto t$) in the long time are indicated by the dashed lines. (b) The plot of time-dependent diffusion coefficient, $D(t)$, as a function of time. Parameters were the same as in Fig. 4.

In the very small ($\epsilon < 0.0075$) and intermediate ($0.05 < \epsilon < 0.07$) roughness regimes, the system is moderately chaotic and for other values of roughness the system is highly chaotic. Comparison of bifurcation diagram and the $\langle v \rangle$ vs ϵ plot (Fig. 6) indicate a strong correlation between the ANM and the weak chaotic dynamics of the system. We plotted the phase-space diagram of the system for the ϵ values corresponding to maximum ANM ($\epsilon = 0.005$ and $\epsilon = 0.06$) and we found that system is weakly chaotic. On the contrary, phase-space plot reveals strongly chaotic dynamics at the roughness ($\epsilon = 0.035$) where the system shows maximum positive velocity. Therefore, weak chaos seems to be the origin of the roughness-induced ANM.

Diffusion anomalies are known to occur in driven inertial Brownian ratchets under smooth periodic potential. Previous studies have indicated the existence of super- and subdiffusive regimes across different time scales of the dynamics [41,45–47]. To determine the nature of diffusion under roughness of the potential, we looked at the mean square displacement, $\langle \Delta x^2(t) \rangle (= \langle [x(t) - \langle x(t) \rangle]^2 \rangle)$, and time-dependent diffusion coefficient, $D(t) (= \langle \Delta x^2(t) \rangle / 2t)$ (Fig. 10). $\langle \Delta x^2(t) \rangle$ versus t plot indicate that the system exhibits ballistic behavior in the early time and normal diffusion is established at a later time. While the smooth system takes a substantially long time to establish normal diffusion, the roughness enforces normal diffusion early. In fact, duration of ballistic phase becomes progressively shorter with increasing roughness. We also plotted the time-dependent diffusion coefficient, $D(t)$, and indeed the smooth system takes a long time to establish normal diffusion where $D(t)$ becomes time independent. These plots clearly show that normal diffusion is established early under roughness. Therefore, these results indicate that the ANM is not a by product of anomalous diffusion of the Brownian system under rough potential.

The role of asymmetry in a periodic potential has been extensively studied in the context of ratchet models as it becomes crucial in breaking spatial symmetry of the system in absence of an external load. Therefore, we looked at the effect of the asymmetry on the ANM in presence of roughness of the periodic potential. To introduce asymmetry in the potential, $U_2(x)$ was added to the $U(x)$ in Eq. (6) [48],

$$U_2(x) = \frac{\Delta}{2} \sin(2\pi x), \tag{8}$$

where Δ is the asymmetry parameter and in absence of an external load it leads to the loss of reflection symmetry of the symmetric periodic potential [40,41]. After dropping the $\hat{}$ notation, the full expression of the potential energy now becomes

$$U(x) = -\sin(x) + \epsilon \cos(\lambda x) + \frac{\Delta}{2} \sin(2\pi x). \tag{9}$$

In Fig. 11 the effect of asymmetric parameter, Δ, on the transport of the particle is presented for different values of ϵ. In the regime of small asymmetry ($\Delta < 0.1$), again roughness leads to ANM. The variation of $\langle v \rangle$ with Δ indicate that the asymmetry in the periodic potential can lead to current reversal both for the smooth and rough systems. Particularly at a small roughness ($\epsilon = 0.001$) the system exhibits multiple current reversals. However, with increased asymmetry the current follows the direction as dictated by the external load. These results indicate that the ANM can be generated in the asymmetric periodic potential as well and the directionality of the current can be tuned by dialing the asymmetric parameter of the potential.

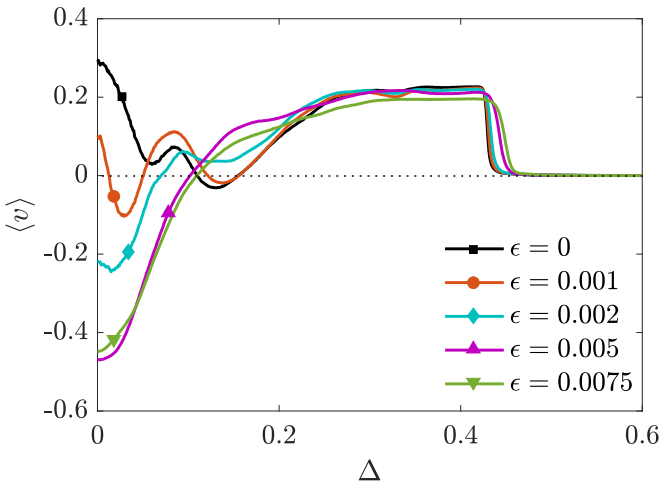

FIG. 11. The plot of $\langle v \rangle$ as a function of asymmetry parameter, Δ, for the indicated values of ϵ with a load $f = 0.03$. Other parameters were $Q = 0.0004$, $\gamma = 0.771$, $a = 1.589$, and $\omega = 0.558$.

IV. CONCLUSION

We have numerically examined how roughness, a microscopic spatial heterogeneity, in a symmetric periodic potential of a driven inertial Brownian ratchet affects the transport characteristics in the presence of an external load. Our main objective was to investigate the consequences of roughness on ANM—an anomalous nature of transport where the direction of the mass transport is opposite to the direction as dictated by the external load. As ANM is sensitive to parameter space [42], we have determined an optimal parameter space where ANM is generated purely due to the roughness in the periodic potential. We show that the roughness-driven ANM is a property of the system in the limit of moderately weak noise. In the quest for finding the dynamic origin of ANM, we found that in presence of roughness the average duration of negative velocity phase is larger than the average duration of the positive velocity phase in the temporal oscillatory dynamics of velocity during a period of the external driving. Therefore, the roughness skews the balance between the negative and positive velocity phases towards negative velocity phase thereby forcing the particle run in the opposite direction of the external load. Furthermore, we find that the system is weakly chaotic in the regime of roughness where ANM is observed indicating a possible connection of weak chaos with the roughness-induced ANM. We show that the roughness-driven anomalous transport is also possible for the system under asymmetric periodic potential where multiple current reversals can be generated as function of asymmetric parameter of the potential.

Charged colloidal particles in microfluidic devices consisting of alternating large and small gaps were shown to generate ANM under periodic external electric field. The periodic physical obstacles with intervening gaps represent periodic potential energy landscape and the microscopic heterogeneity of the gaps sizes were reasoned to be the origin of ANM in such systems [22,23]. Our calculation of roughness-induced ANM can be treated as an example of theoretical consideration of such phenomena. Further recent theoretical work highlighted the role of potential energy function in generating ANM in a driven inertial ratchet [49]. Therefore, our work of roughness-driven ANM falls under the broad consideration of role of potential energy in ANM. Historically, roughness has been considered as the nuisance as it was predicted to be disruptive in barrier crossing dynamics and ratchet transport [35,36]. Our work underscores a constructive role of microscopic spatial heterogeneity in transport properties of driven inertial ratchet and thus can have a potential role in designing mass separation and bioanalytical applications.

ACKNOWLEDGMENTS

The authors acknowledge the Translational Research Facility, UPE-II, School of Chemistry and Center for Modelling Simulation and Design, University of Hyderabad, for computational support.

[1] R. D. Astumian and P. Hänggi, Phys. Today **55**(1), 33 (2002).
[2] P. Reimann, Phys. Rep. **361**, 57 (2002).
[3] P. Reimann and P. Hänggi, Appl. Phys. A **75**, 169 (2002).
[4] P. Hänggi, F. Marchesoni, and F. Nori, Ann. Phys. **14**, 51 (2005).
[5] P. Hänggi and F. Marchesoni, Rev. Mod. Phys. **81**, 387 (2009).
[6] R. Eichhorn, P. Reimann, and P. Hänggi, Phys. Rev. Lett. **88**, 190601 (2002).
[7] L. Machura, M. Kostur, P. Talkner, J. Łuczka, and P. Hänggi, Phys. Rev. Lett. **98**, 040601 (2007).
[8] D. Speer, R. Eichhorn, and P. Reimann, Phys. Rev. E **76**, 051110 (2007).
[9] F. R. Alatriste and J. L. Mateos, Physica A **384**, 223 (2007).
[10] M. Kostur, L. Machura, P. Talkner, P. Hänggi, and J. Łuczka, Phys. Rev. B **77**, 104509 (2008).
[11] L. Machura, M. Kostur, P. Talkner, P. Hänggi, and J. Łuczka, Phys. E **42**, 590 (2010).
[12] L. Machura, J. Spiechowicz, and J. Łuczka, Phys. Scr. **2012**, 014021 (2012).
[13] J. Spiechowicz, J. Łuczka, and P. Hänggi, J. Stat. Mech.: Theory Exp. (2013) P02044.
[14] J. Spiechowicz, P. Hänggi, and J. Łuczka, Phys. Rev. B **90**, 054520 (2014).
[15] J. Spiechowicz, P. Hänggi, and J. Łuczka, New J. Phys. **21**, 083029 (2019).
[16] J.-j. Li, H.-z. Xie, T.-C. Li, and B.-q. Ai, Physica A **560**, 125164 (2020).
[17] R. A. Höpfel, J. Shah, P. A. Wolff, and A. C. Gossard, Phys. Rev. Lett. **56**, 2736 (1986).
[18] B. J. Keay, S. Zeuner, S. J. Allen, K. D. Maranowski, A. C. Gossard, U. Bhattacharya, and M. J. W. Rodwell, Phys. Rev. Lett. **75**, 4102 (1995).
[19] E. H. Cannon, F. V. Kusmartsev, K. N. Alekseev, and D. K. Campbell, Phys. Rev. Lett. **85**, 1302 (2000).

[20] I. I. Kaya and K. Eberl, Phys. Rev. Lett. **98**, 186801 (2007).
[21] J. Nagel, D. Speer, T. Gaber, A. Sterck, R. Eichhorn, P. Reimann, K. Ilin, M. Siegel, D. Koelle, and R. Kleiner, Phys. Rev. Lett. **100**, 217001 (2008).
[22] A. Ros, R. Eichhorn, J. Regtmeier, T. Duong, P. Reimann, and D. Anselmetti, Nature (London) **436**, 928 (2005).
[23] R. Eichhorn, J. Regtmeier, D. Anselmetti, and P. Reimann, Soft Matter **6**, 1858 (2010).
[24] A. Słapik, J. Łuczka, P. Hänggi, and J. Spiechowicz, Phys. Rev. Lett. **122**, 070602 (2019).
[25] A. Słapik, J. Łuczka, and J. Spiechowicz, Phys. Rev. Appl. **12**, 054002 (2019).
[26] A. Słapik and J. Spiechowicz, Sci. Rep. **10**, 1 (2020).
[27] H. Frauenfelder, S. G. Sligar, and P. G. Wolynes, Science **254**, 1598 (1991).
[28] C. Hyeon and D. Thirumalai, Proc. Natl. Acad. Sci. USA **100**, 10249 (2003).
[29] R. Nevo, V. Brumfeld, R. Kapon, P. Hinterdorfer, and Z. Reich, EMBO Rep. **6**, 482 (2005).
[30] A. Heuer, J. Phys.: Condens. Matter **20**, 373101 (2008).
[31] P. Charbonneau, J. Kurchan, G. Parisi, P. Urbani, and F. Zamponi, Nat. Commun. **5**, 3725 (2014).
[32] P. G. Debenedetti and F. H. Stillinger, Nature (London) **410**, 259 (2001).
[33] A. Heuer, B. Doliwa, and A. Saksaengwijit, Phys. Rev. E **72**, 021503 (2005).
[34] T. Linder, B. L. de Groot, and A. Stary-Weinzinger, PLoS Comput. Biol. **9**, e1003058 (2013).
[35] D. Mondal, P. K. Ghosh, and D. S. Ray, J. Chem. Phys. **130**, 074703 (2009).
[36] R. Zwanzig, Proc. Natl. Acad. Sci. USA **85**, 2029 (1988).
[37] Y. Li, Y. Xu, J. Kurths, and X. Yue, Chaos: Interdiscip. J. Nonlin. Sci. **27**, 103102 (2017).
[38] Y. Li, Y. Xu, and J. Kurths, Phys. Rev. E **96**, 052121 (2017).
[39] J. Liu, F. Li, Y. Zhu, and B. Li, J. Stat. Mech.: Theory Exp. (2019) 033211.
[40] G. R. Archana and D. Barik, Phys. Rev. E **104**, 024103 (2021).
[41] J. Spiechowicz, J. Łuczka, and P. Hänggi, Sci. Rep. **6**, 30948 (2016).
[42] M. Wiśniewski and J. Spiechowicz, New J. Phys. **24**, 063028 (2022).
[43] L. Machura, M. Kostur, F. Marchesoni, P. Talkner, P. Hänggi, and J. Łuczka, J. Phys.: Condens. Matter **17**, S3741 (2005).
[44] A. Słapik, J. Łuczka, and J. Spiechowicz, Commun. Nonlinear Sci. Numer. Simulat. **55**, 316 (2018).
[45] J. Spiechowicz and J. Łuczka, Phys. Rev. E **91**, 062104 (2015).
[46] J. Spiechowicz, P. Talkner, P. Hänggi, and J. Łuczka, New J. Phys. **18**, 123029 (2016).
[47] J. Spiechowicz, M. Kostur, and J. Łuczka, Chaos: Interdiscip. J. Nonlin. Sci. **27**, 023111 (2017).
[48] B.-q. Ai and L.-g. Liu, Phys. Rev. E **76**, 042103 (2007).
[49] Y. Luo, C. Zeng, and B.-Q. Ai, Phys. Rev. E **102**, 042114 (2020).